NURETH14-581

DETERMINATION OF MIXING FACTORS FOR VVER-440 FUEL ASSEMBLY HEAD

S. Tóth, A. Aszódi

Institute of Nuclear Techniques, Budapest University of Technology and Economics toth@reak.bme.hu, aszodi@reak.bme.hu

Abstract

CFD models have been developed for the heads of the old, the present and new type VVER-440 fuel assemblies using the experiences of former validation process. With these models, temperature distributions were investigated in typical assemblies and in-core thermocouple signals were calculated. The analyses show that coolant mixing is intensive but not-perfect in the assembly heads. Difference between the thermocouple signal and cross-sectional average temperature at measurement level depends on the assembly type. Using the models, weight factors of the rod bundle regions for the in-core thermocouple have been determined. With these factors, the thermocouple signals were estimated and results were statistically tested using the registered data of the Hungarian nuclear power plant. This test shows that deviations between measured and calculated temperatures can be significantly decreased and consequently monitoring uncertainties can be reduced with using the weight factors.

Introduction

In VVER-440 reactors (Russian designed PWRs), the core outlet temperature field is measured with thermocouples, which are installed above 210 fuel assemblies. These temperatures are important information since they are used to determine the radial distribution of the power and calculate the actual values of the limited parameters in the core monitoring system.

Some years ago, fuel assemblies with increased rod pitch were introduced in the VVER-440 NPPs in order to facilitate the reactor power upgrading. This change caused deviations between the in-core measured and calculated coolant outlet temperatures of the fuel assemblies. Initially, the gamma radiation heating of the thermocouples and their housings was supposed as the main reason of these deviations. Lately, some CFD (Computational Fluid Dynamics) calculations called the attention that the temperature distributions were generally not uniform in the measuring cross-section therefore the thermocouples may not have measured the average values and this fact could lead to the experienced deviations [1], [2], [3]. In order to investigate this problem experimentally, measurements were performed close to operational conditions of the reactors on a full scale test facility in the Kurchatov Institute [4]. The problem was examined with particle image velocimetry as well in the KFKI Atomic Energy Research Institute [5]. These measurements achieved similar conclusions as the CFD simulations.

This issue became rather topical nowadays since introduction of new assembly type with burnable poison is in progress in Hungarian and other VVER-440 NPPs. In order to gather experiences, a CFD model has been developed for the head part of the Kurchatov Institute's test assembly with the code ANSYS CFX [6] and it has been validated based on experimental data [7]. Comprehensive sensitivity studies have been performed for the mesh, the turbulence

model and difference scheme and guidelines have been established for modeling of the VVER-440 assembly heads. Applying the experiences of this validation process, further CFD models have been developed for the heads of the old, the present and new assembly types. With these models, typical fuel assemblies of the core have been investigated.

1. Description of CFD models

In order to analyze the temperature distribution in detail and compute the thermocouple signal, CFD models have been developed for the heads of the old profiled, the present profiled and new burnable poison containing VVER-440 fuel assemblies using the codes ANSYS ICEM and CFX. Experiences of former validation process [7] were utilized during the model developments.

Geometrical structure of each assembly head model is the same. Their dimensions correspond to the dimensions given in their technical documentations. Outer diameter of the rods is 9.1 mm in every case. The rod pitch is 12.2 mm by the old profiled assemblies and 12.3 mm by the present profiled and new burnable poison containing assemblies. Figure 1 shows the model of the heads of profiled fuel assemblies with rod pitch of 12.3 mm. The beginning of the investigated domain is at the end of the fuel bundle's active part and end of the domain is above the in-core thermocouple in the channel of the upper core supporting plate. The model contains all parts of an assembly head that can influence the coolant mixing significantly. Because of meshing reasons, some details are simplified but this can not have considerable effect on calculation of the temperature field and thermocouple signal.

Every model was described with the same hybrid mesh structure (Figure 2). In the lower region close to the spacer gird, a tetrahedral mesh with prismatic near-wall layers was used. Below and above this section, a prismatic mesh with hexahedral near-wall elements was generated. Because of the irregular shape of the upper region, it was described with an unstructured tetrahedral mesh using prismatic layers at the walls. The lower and upper gird regions were connected with a grid interface. Acceptability of the mesh structure and resolution was proven with sensitivity study and comparison to measured data in a pervious work [7]. The girds of various assembly head models consist of about 8.5–9 million elements and 2.8–3 million nodes.

With these models, some old (P2), present (P3) and new type (G) fuel assemblies were studied (Table 1). Investigated old and present type assemblies were used in former cycles of Hungarian NPP's Units 3 and 4 and new type assemblies will be used in a future equilibrium cycle of Unit 4. These assemblies were / will be in the inner positions (_I1 - _I3), in the periphery of the core (_P4, _P5) and next to the control rods (_NC).

The boundary conditions of CFD models were determined with usual load-follow calculations of the NPP [8], which were based on registered operational data by the old, the present fuels and estimated data by the new fuels. C-PORCA neutron physical code was applied to calculate the nodal powers of the pins. Figure 3 shows the pin power distributions in two selected profiled assemblies. Using the nodal powers, the outlet velocities and temperatures of subchannels at the end of the rod bundle's active part were determined with the COBRA code. These velocity and temperature distributions were prescribed at the main inlets of the CFD models. Turbulence intensity (Tu) and viscosity ratio (μ_t/μ) of the inflows were based on the results of former calculations with a rod bundle CFD model [9].

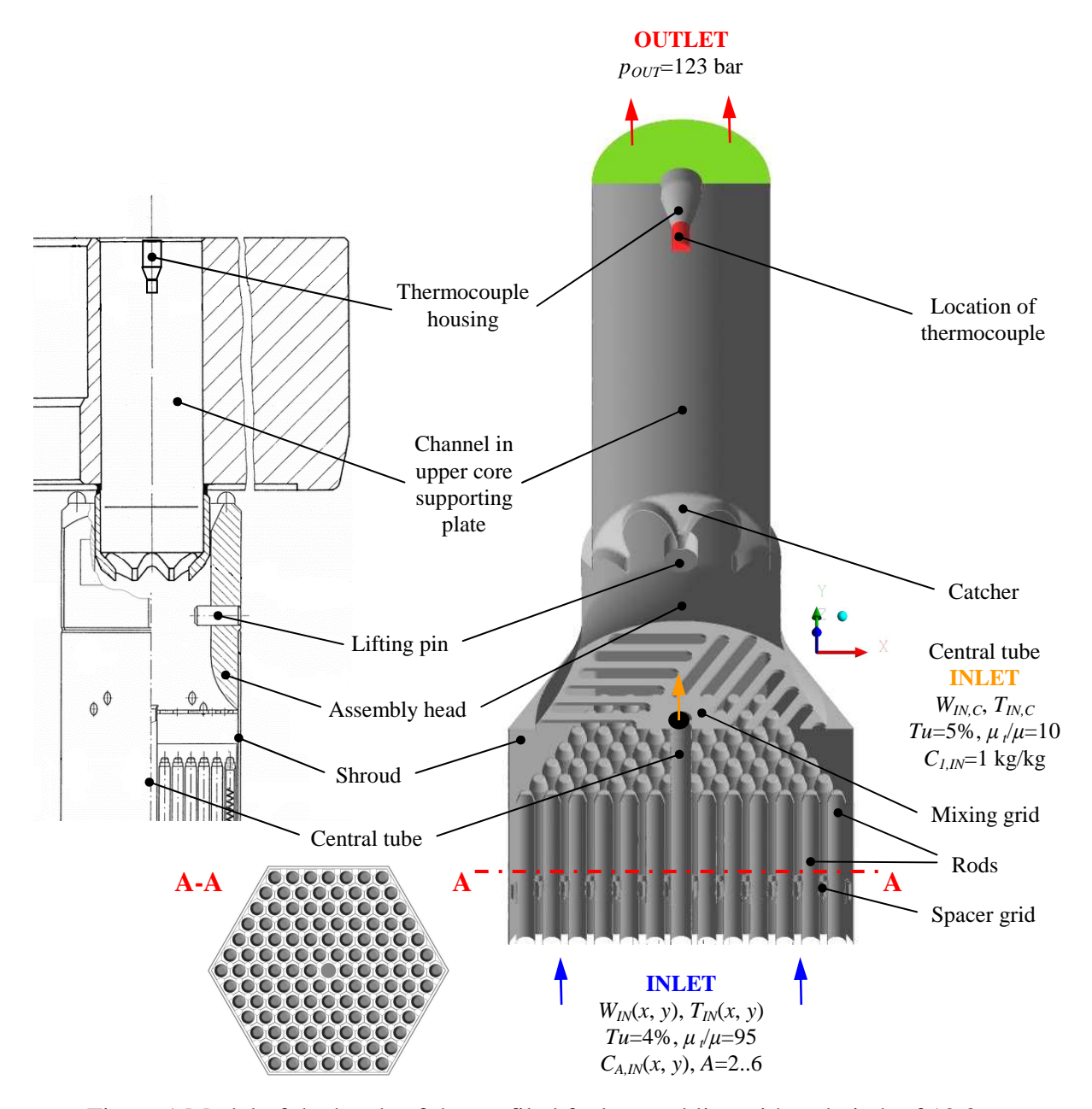


Figure 1 Model of the heads of the profiled fuel assemblies with rod pitch of 12.3 mm (cutaway view).

The central tube flow was modeled as an inlet boundary condition. The mass flow rates and temperatures at the end of the central tube were calculated from correlations, which were determined using data measured on a full-scale test facility [4]. The turbulence quantities were given assuming medium turbulence level.

In order to investigate the contributions of the rod bundle regions to the in-core thermocouple signal, the coolant mixing was analyzed with numerical tracers. Tracer inlets were defined at the end of the central tube and at five regions at the end of the rod bundle's active part (Figure 4). Concentration of a scalar ($C_{A,IN}$) is 1 kg/kg in its entrance region and 0 kg/kg in every other entrance region.

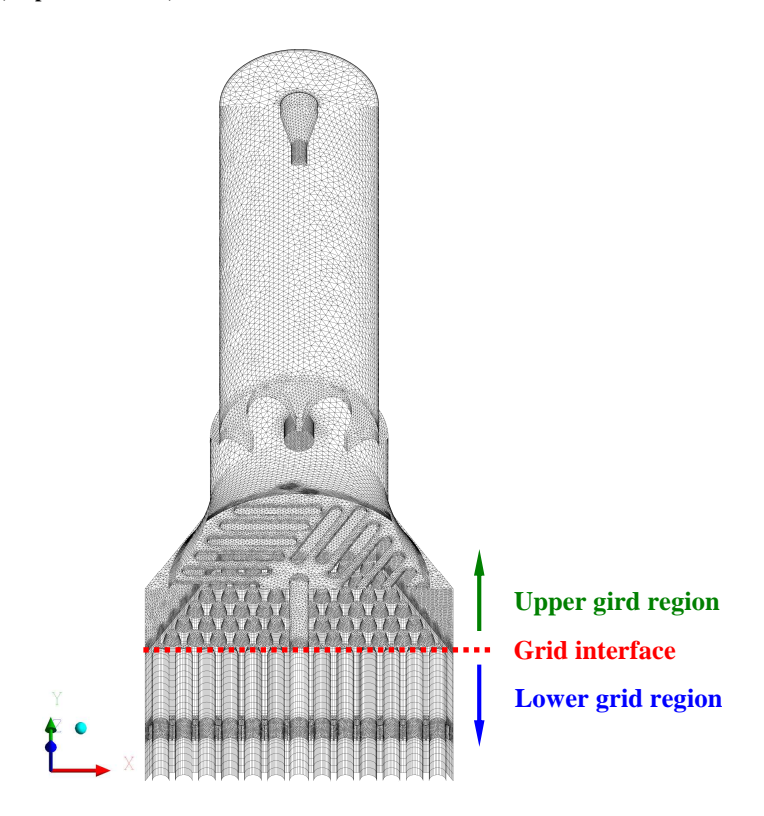


Figure 2 Mesh of the heads of the profiled fuel assemblies with rod pitch of 12.3 mm (cutaway view).

Table 1 Main characteristics of the investigated fuel assemblies.

Туре	Notation	Characteristics	Burnup-cycle	Operational time in cycle [EFPD]	Power [MW]
	P2_I1	Internal	2	223	4.79
3.82% enrichment profiled fuel assemblies, 12.2 mm rod pitch (old type)	P2_I2	Internal	2	223	4.57
	P2_I3	Internal	3	160	4.27
	P2_NC	Next to control assembly	3	223	4.70
	P2_P5	Peripheral, 5 neighbouring assemblies	1	111	3.83
	P2_P4	Peripheral, 4 neighbouring assemblies	1	111	3.06
3.82% enrichment profiled fuel assemblies, 12.3 mm rod pitch (present type)	P3_I1	Internal	1	223	5.59
	P3_I2	Internal	1	223	5.32
	P3_I3	Internal	3	223	4.33
	P3_NC	Next to control assembly	1	223	5.56
	P3_P5	Peripheral, 5 neighbouring assemblies	1	223	3.84
	P3_P4	Peripheral, 4 neighbouring assemblies	1	160	2.80
4.2% enrichment fuel assemblies with Gd, 12.3 mm rod pitch (new type)	G_I1	Internal	1	5	5.40
	G_I2	Internal	2	100	5.32
	G_I3	Internal	4	100	4.28
	G_NC	Next to control assembly	3	100	4.60
	G_P5	Peripheral, 5 neighbouring assemblies	1	5	3.62
	G_P4	Peripheral, 4 neighbouring assemblies	4	100	1.86

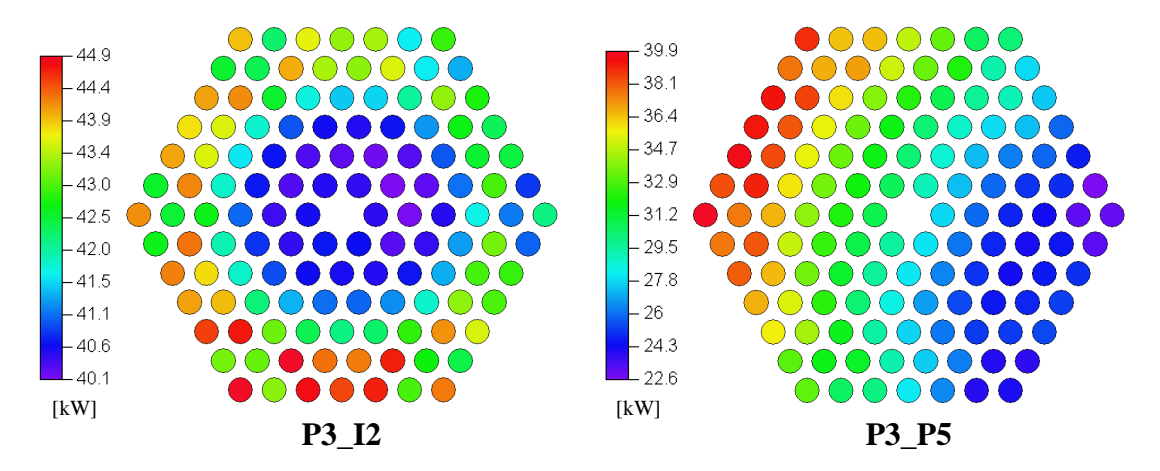


Figure 3 Distributions of the pin powers in two profiled fuel assemblies.

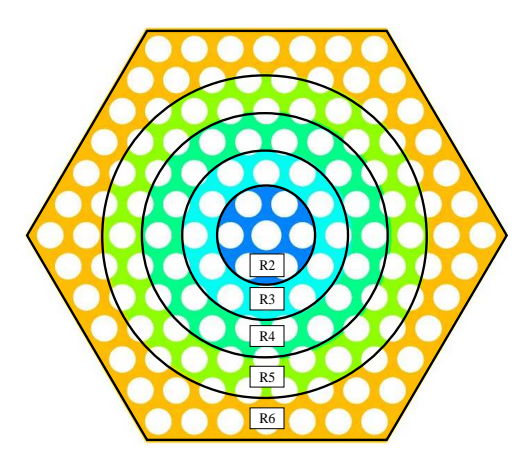


Figure 4 Regions of passive scalars at the inlet of the assembly head models $(C_{A.IN}(x, y), A=2..6)$.

Outlet boundary condition of 0 Pa relative pressure was applied at the upper planes of the models. The reference pressures were 122–123 bar according to the operational data. The physical walls were treated as no-slip, adiabatic walls.

Because of the high Reynolds number of the flow (about 4 million in the channel of the upper core supporting plate) and complexity of the geometry, more sophisticated methods like Large Eddy Simulation (LES) or Detached Eddy Simulation (DES) can not be reasonably applied. The flow was described with the Unsteady Reynolds-Averaged Navier-Stokes (URANS) method. Turbulence was modeled with the BSL Reynolds Stress Model, which was proven to be able to describe the flow field in the VVER-440 assembly heads [7]. In this model, transport equations are solved for six individual Reynolds stresses and specific dissipation of the turbulent kinetic energy. The model is recommended to use in the case of wall-bounded flows that include difficult physical phenomena like strong streamline curvature and secondary eddies.

An additional transport equation (1) was solved for each passive scalar. This equation is consistent with the heat transfer equation for enthalpy if the viscous dissipation is negligible. It describes the change in time, the convection, the molecular diffusion and turbulent transport of a tracer.

$$\frac{\partial \left(\rho \overline{C}_{A}\right)}{\partial t} + \frac{\partial \left(\rho \overline{U}_{j} \overline{C}_{A}\right)}{\partial x_{j}} = \frac{\partial}{\partial x_{j}} \left(\left(\rho D_{A} + \frac{\mu_{t}}{S c_{t}}\right) \frac{\partial \overline{C}_{A}}{\partial x_{j}} \right) \tag{1}$$

where \overline{C}_A is the concentration of tracer 'A', ρ is the density, \overline{U}_j are the velocity components, μ_t is the turbulent viscosity, Sc_t is the turbulent Schmidt number and D_A is the molecular diffusion coefficient of tracer 'A'. Volume-averaged value of thermal diffusivity was given for the values of all diffusion coefficients since investigation of thermal mixing was the goal.

High Resolution Scheme [6] was used in the spatial discretization of the convective terms. Temperature and pressure dependencies of water properties were taken into account using the IAPWS-IF97 formulation, which is implemented in the code.

First, steady-state calculations were performed with the full models. Convergence criteria were 10^{-4} for RMS of the equation residuals. The surface-averaged values of tracer concentrations and temperature on the thermocouple housing (Figure 1, marked by red) were monitored during the calculations as well. Since completely steady-state solutions could be reached neither of these parameters, transient simulations were performed as well using the steady-state results as initial conditions. The region begins 2.5 mm behind the spacer grid was investigated only because it contains the unsteady regions. The steady-state distributions of the velocity components, the turbulence quantities (Reynolds stresses and dissipation), the temperature and tracers' concentrations were given as inlet boundary conditions of the transients. The Second Order Backward Euler Scheme [6] was applied in the time discretization. 10^{-4} convergence criteria were prescribed for RMS of the equation residuals. 0.00125 s time step was used, which resulted 3–4 subiteration per step. The transients were 1-1.5 s long, which were enough to evaluate the time averages of the thermocouple signals within about ± 0.1 °C uncertainty.

2. Velocity and temperature fields in heads of fuel assemblies

The calculations were run using eight INTEL XEON 3000 MHz processors. A steady-state simulation needed about 20 hours and a transient simulation needed about 200 hours wall clock time

Figure 5 shows the instantaneous velocity field of the coolant in the assembly head of a profiled fuel assembly with rod pitch of 12.3 mm. The velocity distributions are similar to this in the cases of other fuel assembly types. Velocity field is relatively uniform in the rod bundle. Behind the rods, in the corners of the shroud and behind the mixing gird, large eddies develop, which cause intensive convective mixing. The flow accelerates in the cuts of the mixing grid because the cross-section decreases. Due to the effect of the catcher, the velocity increases in the middle zone and vertical eddies form in the peripheral region. It can be seen that a complex, three dimensional flow pattern develops in the assembly heads.

Figure 6 shows the time-averaged temperature field in the head of an inner profiled fuel assembly with rod pitch of 12.3 mm (P3_I2). The temperature distribution is nearly symmetrical but inhomogeneous at the end of the rod bundle's active part (at the inlet of the head model) according to the pin power distribution (Figure 3). This character does not change significantly in the inactive rod bundle region.

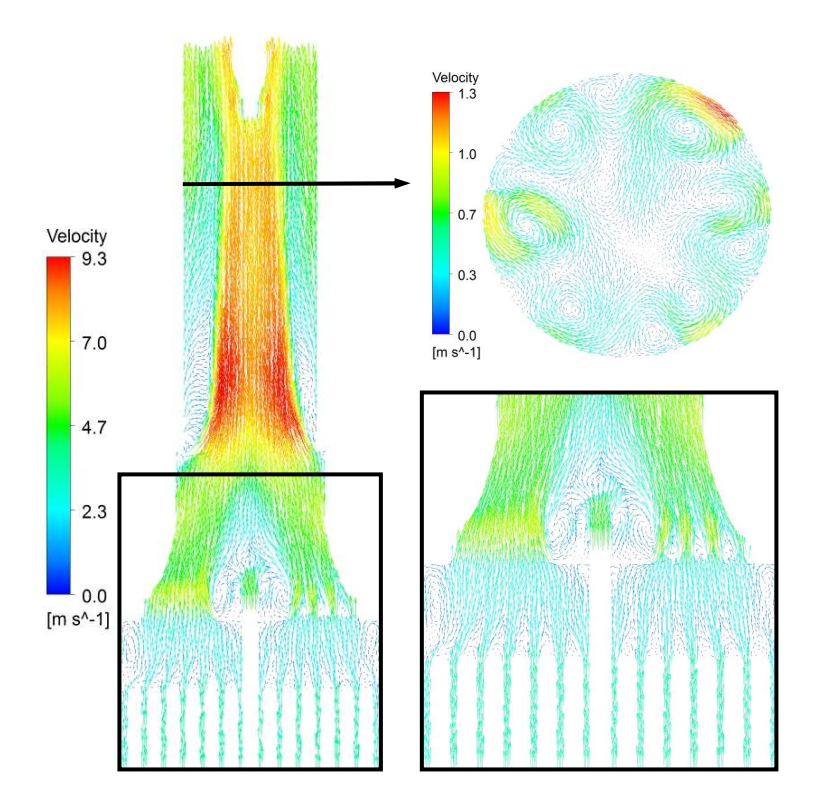


Figure 5 Instantaneous velocity field of the coolant in head of a profiled fuel assembly with rod pitch of 12.3 mm (P3_I2).

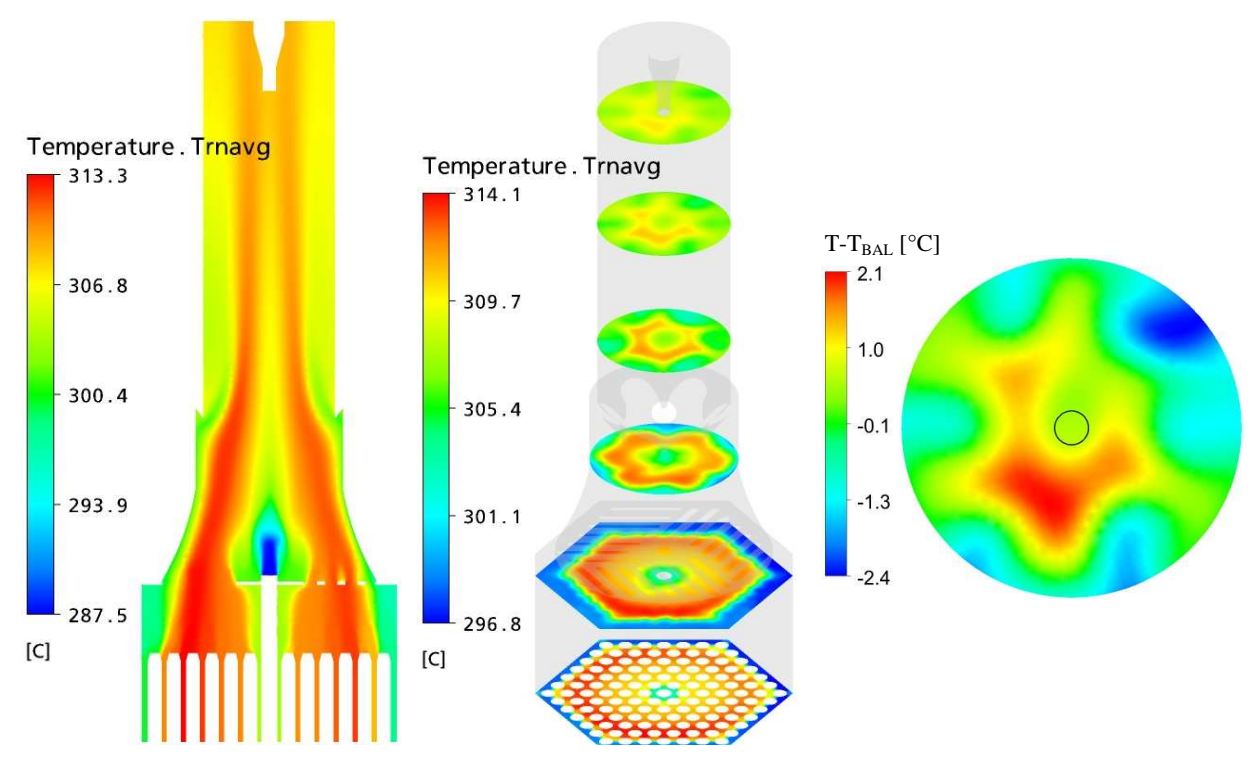


Figure 6 Time-averaged temperature field in the head of a profiled fuel assembly with rod pitch of 12.3 mm, symmetrical pin power distribution (P3_I2).

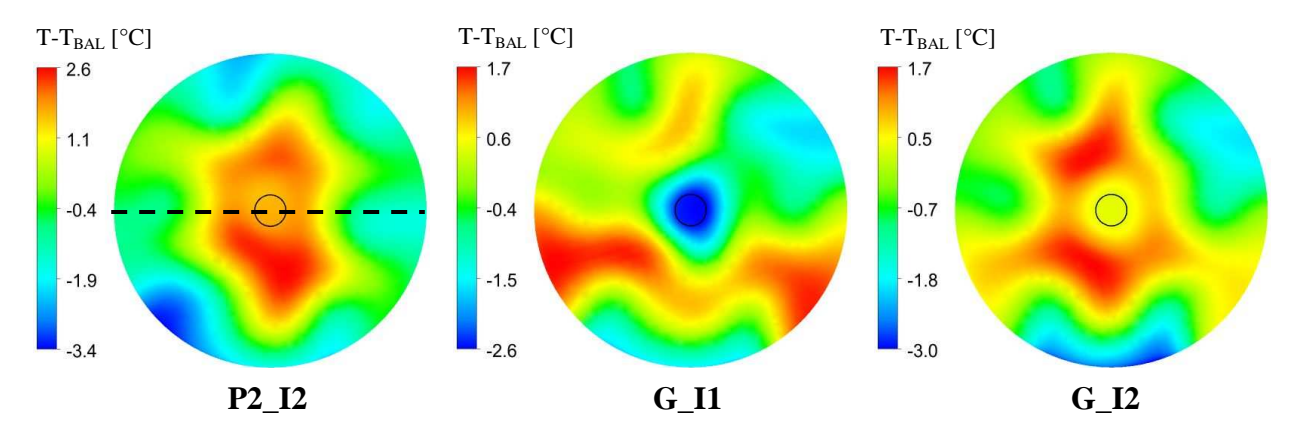


Figure 7 Time-averaged cross-sectional temperature distributions at the level of the thermocouple by different assemblies with symmetrical pin power distributions.

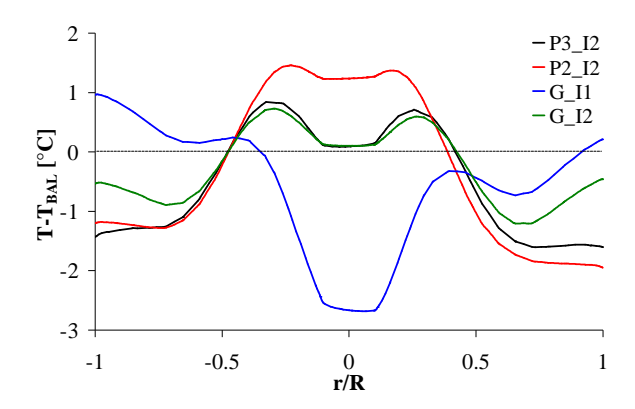


Figure 8 Time-averaged temperature profiles along a line (see Figure 7) at the level of the thermocouple by different assemblies with symmetrical pin power distributions.

Change of the geometry's shape, the mixing grid and catcher intensify the coolant mixing therefore the cross-sectional temperature distribution becomes more uniform downstream. However, the 4–5 L/D long section between the end of the rod bundle and in-core thermocouple location is too short that the coolant can mix perfectly. For this reason, there is near 5 °C difference between the maximum and minimum of the cross-sectional temperature field at the level of the thermocouple. In spite of the non-perfect coolant mixing, the thermocouple measures nearly the cross-sectional average temperature (T_{BAL}) in this case. Main characters of the temperature distributions are similar by other inner fuel assemblies, however the fields at thermocouple level differ significantly (see Figures 7 and 8). By a profiled assembly with rod pitch of 12.2 mm (P2_I2), the coolant temperature at the thermocouple housing is higher than the cross-sectional average value. By a fresh Gd assembly (G_I1), this temperature is significantly lower than the average one and by a Gd assembly with higher burnup (G_I2), it agrees well with the average value. These different behaviors of Gd fuels are caused by the burnup of the Gadolinium from three rods near the assembly centre.

In the case of a peripheral profiled assembly with rod pitch of 12.3 mm (P3_P5), the temperature distribution at the ends of the rods' active part (Figure 9) is rather asymmetrical due to the inclined pin power distribution (Figure 3). This character practically does not change in the inactive rod bundle section. From the end of the rod bundle up to the thermocouple, the

inhomogeneity decreases significantly but about 13 °C difference remains between the extremes of the cross-sectional temperature distribution at the thermocouple level. The temperature fields are similar in the cases of other peripheral fuel assemblies but there are significant quantitative differences between them at the thermocouple level (see Figures 10 and 11). By a profiled assembly with rod pitch of 12.2 mm (P2_P5), temperature at the thermocouple housing is higher than the cross-sectional average value. By a fresh Gd fuel (G_P5), this temperature is significantly lower than the average and by a Gd fuel with higher burnup (G_P4) it corresponds nearly with the mean value.

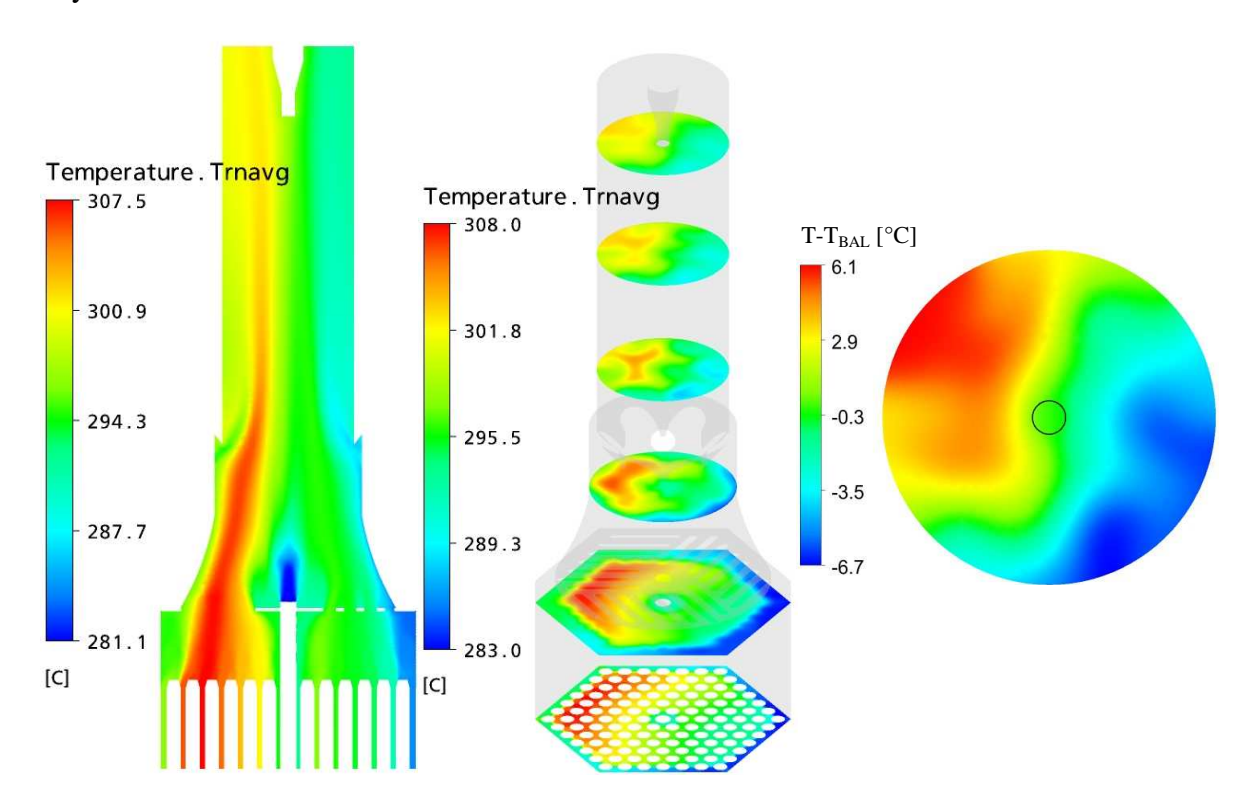


Figure 9 Time-averaged temperature field in the head part of a profiled fuel assembly with rod pitch of 12.3 mm, asymmetrical pin power distribution (P3_P5).

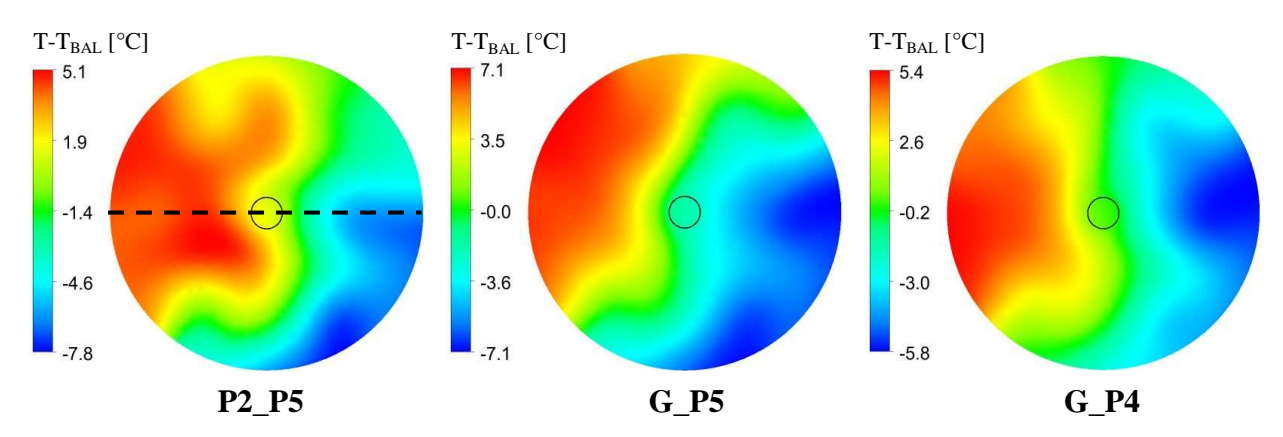


Figure 10 Time-averaged cross-sectional temperature distributions at the level of the thermocouple by different assemblies with asymmetrical pin power distributions.

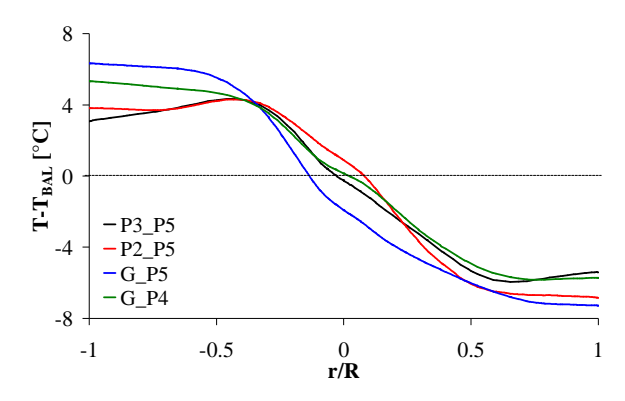


Figure 11 Time-averaged temperature profiles along a line (see Figure 10) at the level of the thermocouple by different assemblies with asymmetrical pin power distributions.

Table 2: Main numerical results of the calculations.

Туре	Notation	T_{BAL}	T_{TC}	T_{TC_M}	T_{TC} - T_{TC_M}	T _{TC} -T _{BAL}	(T T)/AT	
		[°C]	[°C]	[°C]	[°C]	[°C]	$(T_{TC}-T_{BAL})/\Delta T$	
3.82% enrichment profiled fuel assemblies, 12.2 mm rod pitch	P 2_I1	303.8	305.2	306.4	-1.1	1.4	3.8%	
	P 2_I2	302	303.3	303.3	0	1.3	3.6%	
	P 2_I3	301	302.3	303.2	-0.9	1.3	3.6%	
	P2_NC	303.9	305.4	305.8	-0.4	1.4	3.8%	
(old type)	P2_P5	296.1	297	296.8	0.2	0.9	3%	
	P2_P4	290.1	290.9	291.1	-0.1	0.8	3.2%	
3.82% enrichment profiled fuel assemblies, 12.3 mm rod pitch (present type)	P3_I1	310	310.1	310.7	-0.6	0.1	0.3%	
	P3_I2	308.5	308.7	307.7	1	0.2	0.5%	
	P3_I3	300.3	300.6	301.7	-1.1	0.2	0.7%	
	P3_NC	309.4	309.4	308.6	0.8	0	0%	
	P3_P5	297.1	297	296.2	0.8	-0.2	-0.6%	
	P3_P4	289.4	290.1	289.2	0.9	0.6	2.7%	
4.2% enrichment	G_I1	309.4	306.9	-	-	-2.4	-5.8%	
	G_I2	308.9	309.1	-	-	0.1	0.4%	
fuel assemblies with Gd,	G_I3	301.3	301.6	-	-	0.3	1%	
12.3 mm rod pitch (new type)	G_NC	303.7	304.1	-	-	0.4	1.1%	
	G_P5	296.3	294.5	-	-	-1.8	-6%	
	G_P4	282.4	282.6	-	-	0.2	1.1%	

Main numerical results of the calculations are summarized in Table 2. The calculated signals (T_{TC}) agree acceptably with the data measured with the in-core thermocouples (T_{TC_M}) considering the uncertainties and complexity of the problem. The deviations are within ± 1 °C generally. Contact resistant between the thermocouple and its housing, uncertainties in the operational data, measurement and computational errors (neutronics, thermalhydraulics) can contribute to these deviations. The differences between the calculated signals and cross-sectional average temperatures at thermocouple level (T_{BAL}) are negligible in the cases of profiled fuels with rod pitch of 12.3 mm. These differences are between 0.8 and 1.4 °C by profiled fuels with rod pitch of 12.2 mm. The calculated deviation between the behaviors of these assembly types

coincides well with the operational experiences of Hungarian NPP [8]. In the cases of Gd assemblies, the differences between the calculated signals and cross-sectional average temperatures are significantly influenced by the burnup. The deviations are negligible by fuels with higher burnup. Whereas, by fresh Gd fuels these deviations are -2.4 and -1.8 °C, which are about 6% of the average heat ups of the coolant. This result calls the attention that assembly powers can be significantly underestimated if they are simply calculated based on in-core thermocouple signals without using any corrections.

The calculations show that the differences between the in-core thermocouple signals and cross-sectional average temperatures depend on the assembly type and in the cases of Gd fuel assemblies they are influenced by the burnup as well. The monitoring uncertainties can be reduced if the thermocouple signals are estimated in the core analysis system and they are compared to the measured data instead of the calculated average temperatures.

3. Determination and test of weight factors

In order to determine the contributions of the rod bundle regions to the thermocouple signal, the coolant mixing was investigated with numerical tracers. Figure 12 shows the distributions of the tracers in the head of a profiled fuel assembly with rod pitch of 12.3 mm. The fields are rather similar to these in the cases of other investigated assemblies. It can be seen that tracers entering from different rod bundle regions do not mix uniformly in the cross-section up to the thermocouple. Consequently, the coolant mixing is not perfect. The mixing gird and catcher considerably intensify the mixing. The gird influences it in the full cross-section while the catcher has effect on it in the peripheral region mainly. Flows from the central tube and R2, R3, R4 rod bundle regions, accordingly from the inner five subchannel rings influence significantly the thermocouple reading.

Weight factors of the rod bundle regions (δ_A) were evaluated with taking the surface average of the time-averaged tracers' concentrations on the thermocouple housing (2).

$$\delta_{A} = \frac{1}{\sum_{A=1}^{6} C_{A}} \frac{1}{A_{TC}} \frac{1}{\Delta t} \int_{A_{TC}}^{t_{0} + \Delta t} C_{A}(x_{i}, t) dt dA$$
 (2)

where Δt is the averaging time and A_{TC} is the outer surface of the thermocouple housing around the thermocouple (Figure 1, marked by red).

Normalization was necessary because sum of the concentrations overshot with a few percents because of used difference scheme for the advection terms. The enthalpy at in-core thermocouple housing $(h_{TC,\delta})$ can be estimated using the weight factors and average enthalpies of flows from central tube and regions at the end of the rod bundle's active part $(3, h_A)$. The average enthalpies can be calculated with the subchannel code implemented in the core monitoring system. Using the pressure and enthalpy at the thermocouple housing, the signal can be determined: $T_{TC,\delta} = T_{TC,\delta}(h_{TC,\delta}, p)$.

$$h_{TC,\delta} = \sum_{A=1}^{6} \delta_A h_A \tag{3}$$

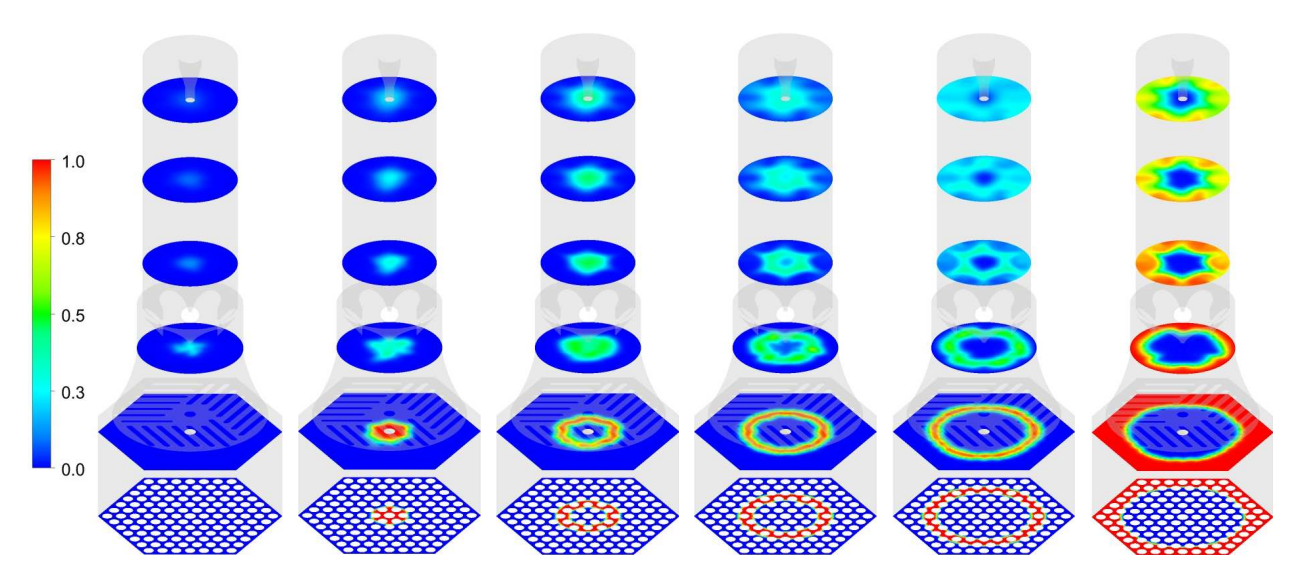


Figure 12 Time-averaged distributions of tracers' concentrations in the head of a profiled fuel assembly with rod pitch of 12.3 mm (P3_I2).

Table 3: Application of the weight factors for fuel assemblies with rod pitch of 12.2 mm.

	P2_I1	P2_I2	P2_I3	P2_NC	P2_P5	P2_P4
$T_{TC,\delta}[^{\circ}C]$	305.4	303.4	302.5	305.5	297.5	291.5
T _{TC} [°C]	305.2	303.3	302.3	305.4	297.0	290.9
$T_{TC,\delta}$ - T_{TC} [°C]	0.2	0.1	0.2	0.1	0.5	0.6
$T_{TC,\delta P3}[^{\circ}C]$	305.3	303.4	302.5	305.4	297.4	291.3
$T_{TC,\delta P3}$ - T_{TC} [°C]	0.1	0.1	0.3	0.1	0.4	0.4

The thermocouple signals were estimated in the cases of all investigated fuel assemblies using their own weight factors ($T_{TC,\delta}$). Results concerning profiled assemblies with rod pitch of 12.2 mm are given in the Table 3. The signals computed with the CFD models (T_{TC}) and signals calculated with the weight factors ($T_{TC,\delta}$) agree well. These differences are not larger than 0.2 °C by assemblies with symmetrical pin power distributions and 0.6 °C by assemblies with asymmetrical pin power distributions. In order to test the generality, the thermocouple signals were determined using the factors of a profiled assembly with rod pitch of 12.3 mm (T_{TC,δ_P3}). Similar results were obtained compared to the results calculated with own factors. In the cases of other fuel assembly types, the same discussion can be made. It can be concluded that weight factors of different assemblies do not differ significantly in terms of the thermocouple signal's estimation. A weight vector can be used for other VVER-440 assemblies within the scope of this investigation.

The weight factors were statistically tested using the registered data of 20th cycle of Hungarian NPP's Unit 4 and results of regular core analysis. In this cycle, profiled assemblies with both 12.2 mm and 12.3 mm rod pitches were in the reactor core in equal shares. The frequency distributions of differences between the measured and calculated temperatures (4) are shown in Figure 13.

$$\Delta T_{TC} = T_{TC_M} - T_{TC} \tag{4}$$

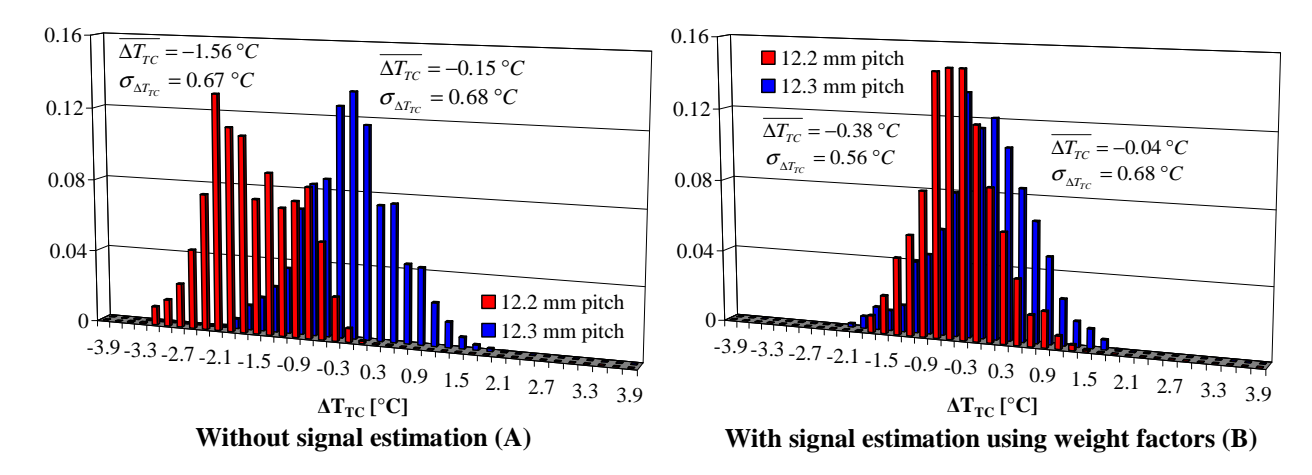


Figure 13 Frequency distributions of differences between the measured and calculated temperatures in the cases of profiled fuel assemblies (20th cycle of Hungarian NPP's Unit 4; 3,000 – 30,000 data pairs) [8], [10].

In the case 'A', perfect coolant mixing was supposed, consequently the calculated average coolant temperatures at the thermocouple level were compared to the measured signals $(T_{TC}=T_{BAL})$. It can be seen that this assumption resulted two different frequency distributions in the cases of two assembly types. The deviation between the means of frequency distributions is about 1.4 °C, which generally agrees well with the deviations between these assembly types experienced in the CFD calculations (Table 2). In the case 'B', the signals were estimated using the weight factors of the P3_NC profiled assembly $(T_{TC}=T_{TC,\delta})$. Due to this estimation, the frequency distributions of different assembly types became similar and difference between their means decreased significantly (to about 0.35 °C). Both means are close to zero. It can be concluded that dependence of the deviations on the fuel assembly type can be eliminated and monitoring uncertainties can be reduced with using the weight factors to estimate the in-core thermocouple signals. Based on these investigations, main reason of formerly experienced deviations between the measured and calculated temperatures is the non-prefect coolant mixing in the assembly heads.

4. Conclusions

Applying the experiences of former validation process, CFD models have been developed for the heads of the old profiled, the present profiled and new burnable poison containing VVER-440 fuel assemblies. The coolant mixing and temperature fields were investigated with these models in some typical assemblies. The in-core measured and calculated thermocouple signals agree acceptably considering the uncertainties and complexity of the problem.

The analyses show that the mixing is intensive but it is not perfect in the assembly heads. The magnitudes of differences between the thermocouple signals and cross-sectional average temperatures at measurement level significantly depend on the fuel assembly type and in the cases of Gd fuel assemblies they are influenced by the burnup as well. These deviations are significant by the old type profiled fuels and by the new type fresh fuels with burnable poison.

The calculated difference between the behaviors of the old and present type profiled assemblies coincides well with the operational experiences of Hungarian NPP.

Coolant mixing in the assembly heads was analyzed with numerical tracers and weight factors of the rod bundle regions for the thermocouple were determined. Based on these investigations, flows from the central tube and inner five subchannel rings influence significantly the thermocouple reading. The thermocouple signals were estimated using the weight factors as well. These estimated signals agree well with the signals determined with the three dimensional CFD simulations. The assembly type and pin power distribution do not influence significantly the weight factors within the scope of this investigation.

The weight factors were statistically tested using the registered data of Hungarian NPP and results of regular core analyses. This test shows that in-core thermocouple signals can be reliably estimated using the factors. The dependence of the deviations on fuel assembly type can be eliminated and monitoring uncertainties can be reduced using them. Based on these investigations, main reason of formerly experienced deviations between the measured and calculated temperatures is the non-prefect mixing in the assembly heads. Implementation of the weight factors in the core monitoring system of Hungarian NPP is in progress.

5. Acknowledgment

This work is connected to the scientific program of the "Development of quality-oriented and harmonized R+D+I strategy and functional model at BME" project. This project is supported by the New Hungary Development Plan (Project ID: TÁMOP-4.2.1/B-09/1/KMR-2010-0002).

6. References

- [1] K. Klučárová, V. Petényi and J. Remiš, "The in-core thermocouple measurement checking of their interpretation correctness", <u>Proceedings of the 14th Symposium of Atomic Energy Research on VVER Reactor Physics and Reactor Safety</u>, Helsinki, Finland, 2004 September 13-17.
- [2] G. Légrádi and A. Aszódi, "Further results on the coolant mixing in fuel assembly head", <u>Proceedings of the 14th Symposium of Atomic Energy Research on VVER</u> Reactor Physics and Reactor Safety, Helsinki, Finland, 2004 September 13-17.
- [3] T. Toppila, V. Lestinen and P. Siltanen, "CFD simulation of coolant mixing inside the fuel assembly top nozzle and core exit channel of a VVER-440 reactor", <u>Proceedings of the 14th Symposium of Atomic Energy Research on VVER Reactor Physics and Reactor Safety</u>, Helsinki, Finland, 2004 September 13-17.
- [4] L.L. Kobzar and D.A. Oleksyuk, "Experiments on simulation of coolant mixing in fuel assembly head and core exit channel of VVER-440 reactor", <u>Proceedings of the 16th Symposium of Atomic Energy Research on VVER Reactor Physics and Reactor Safety</u>, Bratislava, Slovakia, 2006 September 22-29.

- [5] D. Tar, G. Baranyai, Gy. Ézsöl and I. Tóth, "Experimental investigation of coolant mixing in VVER reactor fuel bundles by particle image velocimetry", <u>Proceedings of OECD/NEA & IAEA Workshop Experiments and CFD Code Applications to Nuclear Reactor Safety</u>, Grenoble, France, 2008 September 10-12.
- [6] ANSYS Inc, "ANSYS CFX-Solver Modeling Guide", "ANSYS CFX Solver Theory Guide", 2009.
- [7] S. Tóth and A. Aszódi, "CFD study on coolant mixing in VVER-440 fuel rod bundles and fuel assembly heads", *Nuclear Engineering and Design*, Vol. 240, No. 9, 2010, pp. 2194-2205.
- [8] Zs. Szécsényi and Cs. Szécsényi, "Assembly thermo hydraulic model ASHYMO improvement for VERONA in-core monitoring system", <u>Proceedings of the 19th Symposium of Atomic Energy Research on VVER Reactor Physics and Reactor Safety</u>, Varna, Bulgaria, 2009 September 21-25.
- [9] S. Tóth and A. Aszódi, "Detailed analysis of coolant flow in VVER-440 fuel rod bundle", <u>Proceedings of the 16th Symposium of Atomic Energy Research on VVER Reactor Physics and Reactor Safety</u>, Bratislava, Slovakia, 2006 September 22-29.
- [10] I. Pós and T. Parkó, "Testing of ASHYMO using Paks operational data", <u>AER Working Group C and G Meeting</u>, Tengelic, Hungary, 2009 June 11-12.